Published in final edited form as:
Nanotechnology. 2011 July 1; 22(26): 265101. doi:10.1088/0957-4484/22/26/265101.

Rationally engineered polymeric cisplatin nanoparticle for improved antitumor efficacy

Abhimanyu Paraskar[1], **Shivani Soni**[1], **Sudipta Basu**[1], **J Chitra**[2], **Amarasiriwardena**[2], **Nicola Lupoli**[2], **Shyam Srivats**[1], **Rituparna Sinha Roy**[1], and **Shiladitya Sengupta**[1,2,3,*]

[1]BWH-HST Center for Biomedical Engineering, Harvard Medical School, 65 Landsdowne street, Cambridge, MA 02139, USA

[2]Channing Laboratory, Department of Medicine, Brigham and Women's Hospital, [2]Harvard-MIT Division of Health Sciences and Technology, Harvard Medical School, 65 Landsdowne street, Cambridge, MA 02139, USA

[3]Dana Farber Cancer Institute, Boston, MA, USA

Abstract

The use of cisplatin, a first line chemotherapy for most cancers, is dose-limited due to nephrotoxicity. While, this toxicity can be addressed through nanotechnology, previous attempts at engineering cisplatin nanoparticles have been limited by the impact on the potency of cisplatin. Here we report the rational engineering of a novel cisplatin nanoparticle by harnessing a novel polyethylene glycol-functionalized poly-isobutylene-maleic acid (PEG-PIMA) co-polymer, which can complex with cis-platinum (II) through a monocarboxylato and a coordinate bond. We show that this complex self-assembles into a nanoparticle, and exhibit an IC_{50} = 0.77 ± 0.11μM comparable to that of free cisplatin (IC_{50} = 0.44 ± 0.09 μM). The nanoparticles are internalized into the endolysosomal compartment of cancer cells, and releases cisplatin in a pH-dependent manner. Furthermore, the nanoparticles exhibited significantly improved antitumor efficacy in a 4T1 breast cancer model *in vivo* with limited nephrotoxicity, which can be explained by preferential biodistribution in the tumor with reduced kidney concentrations. Our results suggest that the PEG-PIMA-cisplatin nanoparticle can emerge as an attractive solution to the challenges in cisplatin chemotherapy.

INTRODUCTION

Cisplatin [cis-dichlorodiammineplatinum(II)] is a first or second line therapy for most malignancies, including testicular, ovarian, cervical and small-cell lung cancer [1], and exerts its activity by interfering with transcription and other DNA-mediated cellular functions [2]. It was also shown recently to be effective in triple negative breast cancer [3]. Its clinical use, however, is dose-limited due to systemic toxicity, primarily to the kidney [4]. Consequently, developing an improved cisplatin has been a holy grail in cancer drug discovery. Only two other platinum-based chemotherapeutics, carboplatin [di-amine(1,1-cyclobutadicarboxylato)platinum(II)] and oxaliplatin [(1R,2R)-diaminocyclohexane)oxalate-platinum(II)] have been approved for use in cancer chemotherapy since the clinical introduction of cisplatin. Carboplatin and oxaliplatin have a cyclobutane-1, 1-dicarboxylato and an oxalate respectively as the leaving groups, which chelate the platinum more strongly conferring greater stability to the leaving group-Pt complex unlike the chlorides in cisplatin

*Correspondence: Dr. Shiladitya Sengupta, Brigham and Women's Hospital, Harvard Medical School, 65 Landsdowne street, Cambridge, MA 02139, USA., ssengupta2@partners.org.

[5]. As a result, both carboplatin and oxaliplatin exhibit improved nephrotoxicity profiles but also lesser efficacy than cisplatin [6,7]. We rationalized that this challenge could be addressed by harnessing a nanotechnology-based strategy. It is now well documented that nanoparticles larger than 10 nm avoid renal clearance [8], and thereby could potentially reduce cisplatin nephrotoxicity. Furthermore, it is now well established that nanostructures in the size range of 100 nm preferentially accumulate in the tumor due to the 'enhanced permeability and retention' (EPR) effect, and result in increased drug loading in the tumor [9].

The formulation of cisplatin in nanoparticles has been a challenge arising from its physicochemical characteristics, which makes entrapment difficult [10,11]. For example, a sterically-stabilized liposomal formulation of cisplatin, SPI-77, failed to demonstrate any improvement in clinical efficacy, which could be attributed to retention of cisplatin within the nanoparticle as a result of increased lipid drug ratio [12]. Alternative strategies based on the conjugation of platinum to polymers, for example a PAMAM dendrimer-platinum complex, resulted in 200–550-fold reduction in cytotoxicity [13]. Similarly, AP5280, a N-(2-hydroxypropyl) methacrylamide (HPMA) copolymer-bound platinum was found to exert minimal nephrotoxicity in clinical studies, but was less potent than carboplatin as the platinum is held to an aminomalonic acid chelating agent coupled to the COOH-terminal glycine of a tetra-peptide (GPLG) spacer [14]. In a recent study, Dhar *et al* generated a platinum (IV) complex (*c*,*t*,*c*-[$Pt(NH_3)_2(O_2CCH_2CH_2CH_2CH_2CH_3)_2Cl_2$]) which had sufficient hydrophobicity for encapsulation in PLGA-*b*-PEG nanoparticles, but the prodrug had to be intracellularly processed into cisplatin [15]. To overcome these challenges, we developed a strategy of harnessing a rational approach of engineering a novel polymer inspired by the leaving group of cisplatin, which can complex with Pt.

Materials and Methods

General Experimental Details—CellTiter 96 AQueous One Solution Cell Proliferation Assay [3-(4,5-dimethylthiazol-2-yl)-5-(3-carboxymethoxyphenyl)-2-(4-sulfophenyl)-2H-tetrazolium, inner salt (MTS) assay] reagent was from Promega (Madison, WI). All Polymer solutions were dialyzed in cellulose membrane tubing, types Spectra/Por 4 and Spectra/Por 6 (wet tubing), with mass-average molecular mass cut-off limits of 1000 and 3500 respectively. Operations were performed against several batches of stirred deionized H_2O. Commercially supplied (Sigma, Fluka AG, Aldrich Chemie GmbH) chemicals, reagent grade, were used as received. These included *N*,*N*-Dimethylformamide (DMF), Poly(isobutylene-*alt*-maleic anhydride) and Triethyl amine. ^{1}H NMR and ^{13}C NMR were measured at 500 and 125 MHz, respectively, with a Varion-500 or a Brucker-400 spectrometer. ^{1}H NMR chemical shifts are reported as δ values in parts per million (ppm) relative to either tetramethylsilane (0.0 ppm) or deuterium oxide (4.80 ppm). ^{195}Pt NMR chemical shifts are reported as δ values in parts per million (ppm) relative to Na_2PtCl_6 (0.0 ppm). Carbon-13 chemical shifts are reported in ppm relative to $DMSOd_6$ (39.5 ppm). Starting materials were azeotropically dried prior to reaction as required, and all air- and/or moisture-sensitive reactions were conducted in flame- and/or oven-dried glassware under an anhydrous nitrogen atmosphere with standard precautions taken to exclude moisture.

Synthesis of PIMA-PEG-Cisplatin Nanoparticle

The Poly(isobutylene-*alt*-maleic anhydride) PIMA 1 (3 mg, 0.0005 mmol) and Et_3N (0.021 mL, 0.015 mmol) was dissolved in Dry (10 mL) in 25 mL RB under N_2 and then was added polyethyeneglycol [PEG-NH_2, MW=2KD] (20 mg, 0.01 mmol), the resulting reaction solution was then heated at 80 ºC with continuous stirring for 3 days. The reaction was allowed to cool to room temperature and then water (1 mL) was added and continue stirring for 1 h at 80 ºC. Solvents are removed under vacuum and unreacted PEG-NH_2 of MW 2KD

was removed from required polymer by dialysis. Dialysis was carried out for 5 days using membrane of molecular cut off of 3.5–5KD to give colorless solution which was then lyophilized to give 4 mg white colored PIMA-PEG. ^{1}H-NMR (300 MHz, D_2O) δ 3.5–3.7 (m), 3.0–3.1 (m), 2.5–2.8 (m), 0.7–1.0 (m).

Cisplatin and $AgNO_3$ was added to 10ml double distilled water. The resulting solution was stirred in dark at room temperature for 24h. AgCl precipitates were found after reaction. AgCl precipitates are removed from reaction by centrifugation at 10000 rpm for 10 min. The supernatant was further purified by passing through 0.2μm filter.

The brush polymer PIMA-PEG (0.019 g, 0.00007 mmol) was taken in 10 mL RB flask mixed with aquated cisplatin (0.0002 g, 0.0007 mmol) dissolved in 0.3 mL double distilled water. After stirring for 3 days at room temperature (25 ºC) the resulting turbid reaction mixture was dialyzed. The solution containing PIMA-PEG-cisplatin conjugate was further purified by dialyzing it in cellulose membrane tubing, types Spectra/Por 4 and with mass-average molecular mass cut-off limits of 1000 to remove free cisplatin. PIMA-PEG cisplatin conjugate was then lyophilized to get white colored solid. The conjugate was re-suspended in double distilled water for further experiments.

Synthesis of FITC labeled Cisplatin Nanoparticles—Poly(isobutylene-*alt*-maleic anhydride) PIMA (0.006 g) was dissolved in DMF (5 mL) and then was added a solution of Triethyleneamine (0.042 mL, 0.03 mmol, in DMF) and Polyethyleneglycol [PEG-NH_2, MW=2KD], (20 mg, 0.01 mmol, dissolved in 5 mL dry DMF) the mixture was stirred at 80ºC for 2 days. To the resulting reaction mixture was added 0.0022 g FITC-EDA(FITC-EDA was synthesized by stirring Fluorescein isothiocyanate in excess ethylene diamine at 25ºC for12 h in DMSO) and continue stirring for another 24 h, reaction mixture was quenched by adding double distilled water (1mL). The organic solvent was evaporated under vacuum. The resulting orange solid was purified by dialysis for 3 days using dialysis bag of molecular cut off of 3.5–5KD. Lyophilization gave fluorescent orange PIMA-PEG-FITC polymer. To this FITC labeled polymer PIMA-PEG-FITC (0.004 g) was added 1ml double distilled water containing cisplatin (0.001 g) and then the solution was stirred at room temperature(25°C) for48h. The PIMA-PEG-FITC-cisplatin conjugate formed in solution was further purified by dialysis to remove unattached cisplatin with mass-average molecular mass cut-off was limits of 1000. Lyophilization of the dialyzed solution resulted in orange colored FITC labeled PIMA-PEG-FITC-cisplatin conjugate nanoparticles.

Particle Size Measurement—High resolution TEM images were obtained on a JEOL 2011 high contrast digital TEM. Samples were prepared on lacy carbon 300 mesh copper grids (Electron Microscopy Sciences) by adding drops of aqueous nanoparticles at different concentrations, and allowed to air-dry. The size distribution of nanoparticles was studied by dynamic light scattering (DLS), which was performed at 25 °C on a DLS-system (Malvern Zetasizer) equipped with a He Ne laser.

Physicochemical Release Kinetics Studies—Concentrated PIMA-PEG-cisplatin conjugate was resuspended into 100 μL of double distilled water and transferred to a dialysis tube (MWCO: 1000 KD, Spectrapor). The dialysis tube was put into a tube containing magnetic pellet and 2 mL solutions of different pH 8.5 and 5.5. Different pH of the solutions is adjusted by mixing different ratio of 1N sodium hydroxide and 1N nitric acid in water. Cisplatin release was studied by gently stirring the dialysis bag at 300 rpm using IKA stirrer at 25 ºC. 10μL aliquots were taken from the outside solution of dialysis membrane bag at predetermined time intervals and subjected to next UV-Vis active complex of formation reaction by adding 100 μL of ortho-phenyldiamine (1.2 mg/ml in DMF) and heating the resulting solution up to 3h for further UV-Vis analysis (Shimadzu UV 2450). 10 μL of fresh

solution was put back to outside solution of dialysis membrane bag to maintain same concentration. The amount of the drug that was released was evaluated by UV-spectrophotometer (Shimadzu UV 2450) at 706 nm by diluting 10 times it with DMF.

***In Vitro* Cell Culture and Cell Proliferation Assay—**The Breast Cancer cell line (4T1) was purchased from American Type Culture Collection (ATCC, Rockville, MD, USA). 4T1 cells are cultured in RPMI medium supplemented with 10% FBS, 50unit/ml penicillin and 50unit/ml streptomycin. Trypsinized cultured 4T1 cancer cell lines were washed twice with PBS and seeded into 96-well flat bottomed plates at a density of 2×10^3 cells in100 μl of medium. They were tested in triplicate in the same 96-well plate for each experiment, as well as of cells and medium alone. The plates were then incubated for 48 h in a 5% CO_2 atmosphere at 37ºC. The cells were washed and incubated with 100 μl phenol-red free medium (without FBS) containing 20 μl of the CellTiter 96 Aqueous One Solution reagents (Promega, WI, USA). This assay [3- (4,5-dimethylthiazol-2-yl)-5-(3-carboxymethoxyphenyl)-2-(4-sulfophenyl)-2H-tetrazolium, inner salt] (MTS) is a colorimetric method for determining the number of viable cells in proliferation or cytotoxicity assays. After 2-h incubation in a 5% CO_2 atmosphere at 37ºC, the absorbance in each well was recorded at490 nm using a VERSA max plate reader (Molecular Devices, Sunnyvale, CA, USA). The absorbance reflects the number of surviving cells. Blanks were subtracted from all data and results analyzed using GraphPad Prism software (GraphPad, San Diego, CA). The mean of absorbance data in triplicate for each tested dose from three independent experiments was divided by the mean of untreated control cells. The log of thequotient was used to plot a graph as a function of given dose, i.e. Y = (Tested Absorbance Mean-Background)/(Untreated Absorbance Mean-Background) vs. X = tested dose.

FACS Analysis—Cells were grown in 6-well plates incubated in the presence of cisplatin nanoparticle and free Cisplatin at 37°C for 24 h at submaximal doses equivalent to 1μM of platinum concentration. After 24 h, the cells were washed with PBS and collected at 0°C. The cells were then treated with annexin V-Alexa Fluor 488 conjugate (Molecular Probes, Invitrogen) and incubated in the dark, at room temperature, for 15 min. The cells were then washed with PBS and incubated with propidium iodide (PI) solution (50 mg/mL; Sigma) containing RNase (1 mg/mL; Sigma). The cell suspensions were then transferred to FACS tubes and analyzed for AnnexinV/PI staining on a BD FACS Calibur instrument. Data were analyzed using a CellQuestPro software (BD Biosciences).

Cellular Uptake Studies—4T1 cells were seeded on glass coverslips in 24-well plates, 50000 cells per well. When cells reached 70% confluency, they were treated with fluorescein (FITC)-conjugated cisplatin nanoparticles for different durations of 30 min, 2 h, 6 h, 12 h, and 24 h, respectively. For colocalization studies, at indicated time points, the cells were washed with PBS and incubated with Lysotracker Red (Molecular Probes) at 37°C for 30 min to allow internalization. The cells were then fixed with 4% paraformaldehyde for 20 min at room temperature, then washed twice with PBS and mounted on glass slides using Prolong Gold Antifade Reagent (Molecular Probes). Images were obtained using a Nikon Eclipse TE2000 fluorescence microscope equipped with green and red filters for fluorescein and Lysotracker Red, respectively.

***In Vivo* 4T1 Breast Cancer Tumor Model—**The 4T1 Breast Cancer cells (3×10^5) were implanted subcutaneously in the flanks of 4-week-old BALB/c mice (weighing 20 g, Charles River Laboratories, MA). The drug therapy was started after the tumors attained volume of 50 mm^3 The tumor therapy consisted of administration of free cisplatin and cisplatin nanoparticle. The formulation was prepared and validated such that 100 μL of cisplatin nanoparticle and free cisplatin contained 3 mg/kg of cisplatin (administered by tail vein

injection). PBS (100 μL) administered by tail-vein injection was used as a control for drug treatment. Each animal received five doses of free drug or cisplatin nanoparticle every alternate day. The tumor volumes and body weights were monitored on a daily basis. The animals were sacrificed when the average tumor size of the control exceeded 4000 mm^3 The tumors were harvested immediately following sacrifice and stored in 10% formalin for further analysis. All animal procedures were approved by Harvard institutional IUCAC committee.

Biodistribution studies—Tumor bearing animals were treated with cisplatin or cisplatin nanoparticles as described above. The tumors and organs were then weighed and dissolved in conc. HNO_3 followed by heating at 100ºC for 12h. To these mixtures 30% H_2O_2 was added, the resulting solutions were stirred for 24h at room temperature and then heated for another 12h to evaporate the liquids. All solid residues were re-dissolved in 1mL water and then amount of platinum was measured by inductively coupled plasma-atomic absorption spectrometry.

Histopathology and TUNEL assay (Apoptotic assay)—The tissues were fixed in 10% formalin and blocks were paraffin embedded, sectioned, and stained with H&E using the core facility of Harvard Medical School for looking at gross histopathological changes following treatment. Tumor and Kidney paraffin sections were further probed for apoptosis or cell death. The sections were deparaffinized and stained with standard fluorescent terminal deoxynucleotidyl transferase-mediated dUTP nick end labeling (TUNEL) staining as a marker for apoptosis by following the manufacturer's protocol (In Situ Cell Death Detection Kit, TMR Red, Roche). Images were obtained using a Nikon Eclipse TE2000 fluorescence microscope equipped with red filter.

Statistical Analysis—Data were expressed as means ± S.D. (*n* 3). Statistical analysis was conducted using the GraphPad Prism software (GraphPad, San Diego, CA). The statistical differences between two groups studied were determined by ANOVA followed by Newman Keuls Post Hoc test. $p < 0.05$ was considered to indicate significant differences.

RESULTS AND DISCUSSION

Cisplatin gets rapidly activated through intracellular aquation of the chloride leaving groups to form *cis*-$[Pt(NH_3)_2Cl(OH_2)]^+$ and *cis*-$[Pt(NH_3)_2(OH_2)]^{2+}$, following which Pt forms covalent bonds to the N7 position of purine bases to form prevalent GpG and ApG intrastrand and interstrand crosslinks. In comparison, carboplatin has a dicarboxylato moiety as the leaving group, which chelate the platinum more strongly [5]. Interestingly, hydrolysis of poly-isobutylene-maleic anhydride (Fig.1)), comprising of 40 units of maleic acid linked linearly through an isobutylene linker, resulted in the generation of poly-isobutylene-maleic acid [PIMA], where each monomer can be complexed to *cis*-$[Pt(NH_3)_2(OH_2)]^{2+}$ through dicarboxylato linkages. As expected, this complex exhibited an IC_{50} value higher than cisplatin *in vitro* consistent with the stable dicarboxylato bonds [16]. To increase the efficacy of the nanoparticles, we, rationalized that derivatizing the polymer with biocompatible polyethylene glycol (PEG) to generate a PIMA-PEG conjugate (Fig.1), that can complex with Pt [Fig.1] via a mixture of di- and mono-carboxylato bond and a coordinate bond, which should release Pt more easily unlike the case of the dicarboxylato linkages. We observed at a Pt:Polymer ratio of 10:1, the complex self assembles into a nanoparticle of 80–140 nm size as observed with transmission electron microscopy (Fig.1B) and quantified by dynamic laser light scatter (Fig.1C). The total loading of platinum was 15±5 μg/mg of polymer. To test the release of Pt from the nanoparticles, we incubated the nanostructures at pH 5.5 in a dialysis membrane, mimicking the acidic pH of the endolysosomal compartment of the tumor. We also selected pH8.5 as a reference pH in the

alkaline range. As shown in Fig.1D, PIMA-PEG-cisplatin nanoparticles resulted in a sustained release of cisplatin at pH5.5 monitored over a 3 days. In contrast the release at pH8.5 was significantly lower, indicating a pH-dependent release of Pt.

To elucidate the mechanism of uptake of the nanoparticles into tumor cells, we labeled the nanoparticles by complexing PIMA-PEG with fluorescein. The cells were incubated with the nanoparticles for defined time periods, following which they were stained with Lysotracker Red that labels the endolysosomal compartment. As shown in Fig.2A, significant internalization was observed within 12 h, with localization in the endolysosomal compartment evident till 24 h. We next evaluated the efficacy of the nanoparticle against a 4T1 breast cancer cell line *in vitro*. As shown in Fig.2B, treatment with the empty polymer had no cytotoxic effects on the cells as quantified using a tetrazolium-based viability assay. Interestingly, both free cisplatin and the PIMA-PEG-cisplatin nanoparticles exhibited similar cell kill at 48 hours post-incubation, with an IC_{50} of 0.44±0.09μM and 0.77±0.11μM respectively. It is however interesting to note that at 48 h time point, only about 40% of the active platinum is released from the nanoparticle (Fig. 1D), indicating that the nanoparticle enhances the effective efficacy, potentially through sustained release to achieve a metronomic dosing effect.

To elucidate the mechanism of cell death, we labeled the drug-treated cells with FITC-labeled Annexin V, which binds to phosphatidylserine that are externalized on cell surface of apoptotic cells. The cells were counterstained with propidium iodide that labels the nucleus of late apoptotic and necrotic cells. As seen in Fig.3, treatment with both PIMA-PEG-cisplatin nanoparticles and free cisplatin induces comparable apoptosis and necrosis of the tumor cells. In contrast, carboplatin at an equivalent Pt concentration was found to be less effective in inducing cell death. This is consistent with previous reports [6] and can potentially be explained by the difference in their rate of activation. In an elegant study, Davies *et al [*17] used a 1H-13N HSQC NMR spectroscopy to demonstrate that aquation of cisplatin results in the rapid formation of active species *cis*-$[Pt(NH_3)_2Cl(OH_2)]^+$ and *cis*-$[Pt(NH_3)_2(OH_2)]^{2+}$ with a rate constant of $8 \times 10^{-5} s^{-1}$. In contrast the rate constant for aquation of carboplatin was found to be 7.2×10^{-7} s^{-7}. This difference in their rate of activation was matched by their rates of binding to DNA [5,6]. This was further validated in our previous study, where the complexation of a non-pegylated PIMA polymer with cisplatin resulted in an IC_{50} comparable to that of carboplatin consistent with the dicarboxylato-bonds between the polymer and the Pt, indicating the introduction of the (O→Pt) coordinate bond following pegylation of PIMA is critical to the improvement in efficacy of the nanoparticle.

We next evaluated the nanoparticles in an *in vivo* 4T1 syngeneic breast cancer model. Tumor-bearing animals were randomized into three treatment groups, and received 5 doses of free or nanoparticle cisplatin (equivalent to 3mg/kg dose of cisplatin). As seen in Fig.4A, treatment with the nanoparticle resulted in significant tumor ablation as compared with the free drug and vehicle-control. TUNEL-labeling the tumor cross section revealed significant apoptosis following cisplatin and cisplatin nanoparticle treatment (4B). We next evaluated the distribution of platinum in the tumor as compared with major organs of the reticuloendothelial system. As shown in Fig.4C, the platinum concentrations in the liver was significantly (P=0.0433) lower in the cisplatin nanoparticle treated group as compared to the free drug, while the concentrations in the lungs and spleen (P=0.0856 and 0.1470 respectively) although exhibited a lower trend with the cisplatin nanoparticle but were statistically not significant. Interestingly, treatment with cisplatin nanoparticles resulted in significantly increased platinum concentration in the tumor as compared with free drug (P=0.0432). This is consistent with previous observations where pegylated nanoparticles in the size range 80–200 nm have been shown to preferentially accumulate into the tumor as a

result of the enhanced permeability and retention effect and enhanced circulation half life arising from reduced clearance by the reticuloendothelial system [9]. Excitingly, the concentration of platinum in the kidney was found to be statistically significantly lower in the cisplatin nanoparticle-treated animals as compared to free cisplatin (P= 0.0394), consistent with the observation that nanoparticles greater than 10 nm hydrodynamic diameter are not cleared by the kidney [8].

Interestingly, as shown in Fig.5A–B, while treatment with the free cisplatin resulted in a significant reduction in the kidney and spleen weights, the cisplatin-nanoparticles had minimal toxicity. While the concentration of platinum achieved in the spleen following administration of free cisplatin or cisplatin nanoparticle were statistically insignificant, the minimal splenic toxicity with the latter could potentially arise from the sustained release of activated platinum. The effect of metronomic dosing on splenic toxicity remains to be dissected. The pathological examination of the kidney tissue cross sections however revealed tubular necrosis following free cisplatin treatment while the nanoparticle induced minimal nephrotoxicity, correlating with the platinum concentrations achieved in the kidney following these treatments. These results were validated with TUNEL staining, which labels cleaved DNA as a marker for early apoptosis, demonstrating that free cisplatin induces tubular apoptosis unlike the cisplatin-nanoparticle (Fig.5C).

In conclusion, we demonstrate that the rational introduction of an O→Pt coordinate linkage following pegylation of the PIMA polymer facilitates rapid but sustained release of platinum in a pH-dependent manner, resulting in an IC_{50} value comparable to that of free cisplatin *in vitro*. Interestingly, the nanoparticle exhibited superior antitumor efficacy as compared with free cisplatin, which can be explained by well established EPR-effect and the potential contribution of pegylation towards increased circulation time that results in preferential accumulation of nanoparticles in the tumor. Additionally, the reduced nephrotoxicity is consistent with reported data in the literature that nanoparticles greater than 10 nm are not cleared by the kidney.

Despite the development of targeted therapeutics [18], cytotoxic chemotherapeutics are still the first line therapy for all tumors. We report that the rational engineering of a polymer inspired by the bioactivation of cisplatin enables the engineering of a novel nano-cisplatin, which offers the possibility of increasing the maximal tolerated dose of cisplatin by improving its therapeutic index. The clinical familiarity of using an established and globally used chemotherapeutic, together with the low cost of the basic building blocks used in fabricating the nanoparticle, can facilitate the rapid translation of this technology.

Acknowledgments

S. Sengupta is supported by US Department of Defense (DOD) Breast Cancer Research Program (BCRP) Era of Hope Scholar Award (W81XWH-07-1-0482), a DOD Collaborative Innovator Grant, and National Institutes of Health Grant R01 (1R01CA135242-01A2). A.P. is supported by a BCRP postdoctoral fellowship award (W81XWH-09-1-0728). S.B is supported by a Charles A King Trust fellowship.

References

1. Kelland L. The resurgence of platinum-based cancer chemotherapy. Nat Rev Cancer. 2007; 7:573. [PubMed: 17625587]
2. Jamieson ER, Lippard SJ. Structure, Recognition, and Processing of Cisplatin-DNA Adducts. Chem Rev. 1999; 99:2467. [PubMed: 11749487]
3. Leong CO, Vidnovic N, DeYoung MP, Sgroi D, Ellisen LW. The p63/p73 network mediates chemosensitivity to cisplatin in a biologically defined subset of primary breast cancers. J Clin Invest. 2007; 117:1370. [PubMed: 17446929]

4. Madias NE, Harrington JT. Platinum nephrotoxicity. Am J Med. 1978; 65:307. [PubMed: 99034]
5. Hongo A, Seki S, Akiyama K, Kudo T. A comparison of in vitro platinum-DNA adduct formation between carboplatin and cisplatin. Int J Biochem. 1994; 26:1009. [PubMed: 8088411]
6. Knox RJ, Friedlos F, Lydall DA, Roberts JJ. Mechanism of cytotoxicity of anticancer platinum drugs: evidence that cis-diamminedichloroplatinum(II) and cis-diammine-(1,1-cyclobutanedicarboxylato)platinum(II) differ only in the kinetics of their interaction with DNA. Cancer Research. 1986; 46:1972. [PubMed: 3512077]
7. Go RS, Adjei AA. Review of the comparative pharmacology and clinical activity of cisplatin and carboplatin. Journal of Clinical Oncology. 1999; 17:409. [PubMed: 10458260]
8. Choi HS, Liu W, Misra P, Tanaka E, Zimmer JP, Itty Ipe B, Bawendi MG, Frangioni JV. Renal clearance of quantum dots. Nat Biotechnol. 2007; 25:1165. [PubMed: 17891134]
9. Moghimi SM, Hunter AC, Murray JC. Long-circulating and target-specific nanoparticles: theory to practice. Pharmacol Rev. 2001; 53:283. [PubMed: 11356986]
10. Avgoustakis K, Beletsi A, Panagi Z, Klepetsanis P, Karydas AG, Ithakissios DS. PLGA-mPEG nanoparticles of cisplatin: in vitro nanoparticle degradation, in vitro drug release and in vivo drug residence in blood properties. J Controlled Release. 2002; 79:123.
11. Fujiyama J, Nakase Y, Osaki K, Sakakura C, Yamagishi H, Hagiwara A. Cisplatin incorporated in microspheres: development and fundamental studies for its clinical application. J Controlled Release. 2003; 89:397.
12. White SC, Lorigan P, Margison GP, Margison JM, Martin F, Thatcher N, Anderson H, Ranson M. Phase II study of SPI-77 (sterically stabilised liposomal cisplatin) in advanced non-small-cell lung cancer. Br JCancer. 2006; 95:822. [PubMed: 16969346]
13. Haxton KJ, Burt HM. Polymeric drug delivery of platinum-based anticancer agents. J Pharm Sci. 2009; 98:2299. [PubMed: 19009590]
14. Lin X, Zhang Q, Rice JR, Stewart DR, Nowotnik DP, Howell SB. Improved targeting of platinum chemotherapeutics. the antitumour activity of the HPMA copolymer platinum agent AP5280 in murine tumour models. Eur J Cancer. 2004; 40:291. [PubMed: 14728945]
15. Dhar S, Gu FX, Langer R, Farokhzad OC, Lippard SJ. Targeted delivery of cisplatin to prostate cancer cells by aptamer functionalized Pt(IV) prodrug-PLGA-PEG nanoparticles. Proc Natl Acad Sci USA. 2008; 105:17356. [PubMed: 18978032]
16. Paraskar AS, Soni S, Chin KT, Chaudhuri P, Muto KW, Berkowitz J, Handlogten MW, Alves NJ, Bilgicer B, Dinulescu DM, Mashelkar RA, Sengupta S. Harnessing structure-activity relationship to engineer a cisplatin nanoparticle for enhanced antitumor efficacy. Proc Natl Acad Sci USA. 2010; 107:12435. [PubMed: 20616005]
17. Davies MS, Berners-Price SJ, Hambley TW. Slowing of cisplatin aquation in the presence of DNA but not in the presence of phosphate: improved understanding of sequence selectivity and the roles of monoaquated and diaquated species in the binding of cisplatin to DNA. Inorg Chem. 2000; 39:5603. [PubMed: 11151361]
18. Shawver LK, Slamon D, Ullrich A. Smart drugs: tyrosine kinase inhibitors in cancer therapy. Cancer Cell. 2002; 1:117. [PubMed: 12086869]

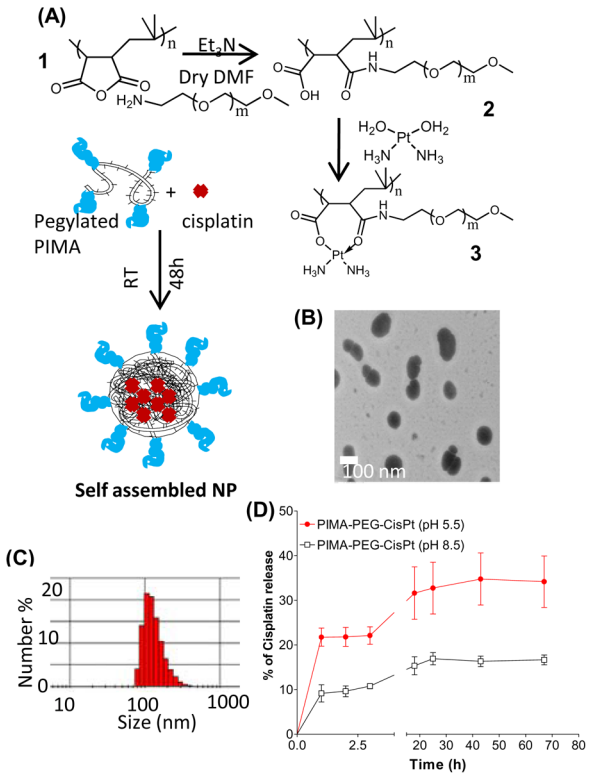

Figure 1.

Engineering and characterization of a Cisplatin nanoparticle. (A) Scheme shows the synthetic steps for PIMA-PEG copolymer and its complexation with $Pt(NH_3)_2(OH_2)]_{2+}$ to self-assemble into a nanoparticle. (B) Representative transmission electron micrograph PIMA-PEG-cisplatin nanoparticle. (C) Representative DLS plot showing distribution of the particle size. (D) Release kinetics of Pt from the nanoparticles as a function of time and pH. Data shown are mean ± SEM from n=3 independent experiments.

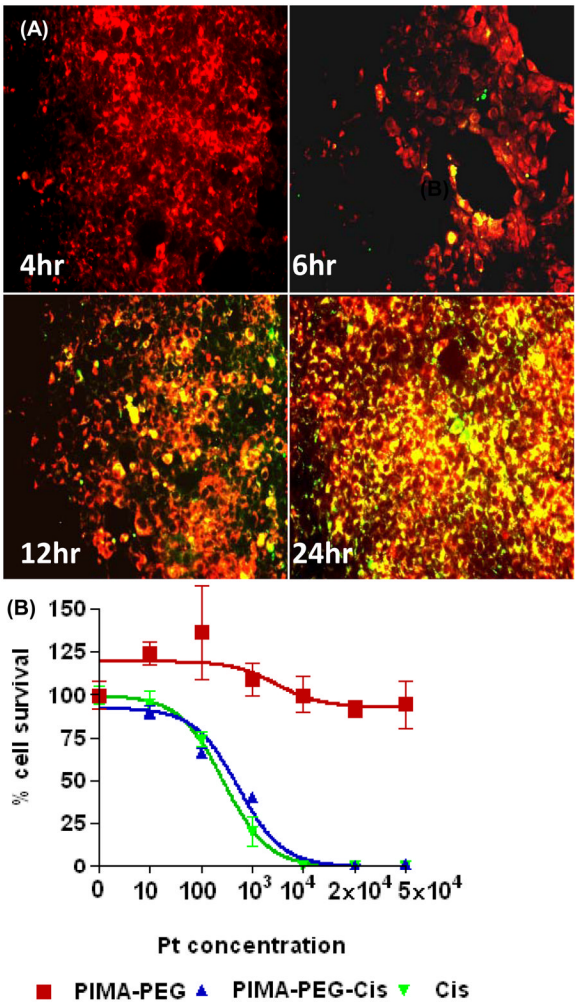

Figure 2.

In vitro characterization of PIMA-PEG-cisplatin nanoparticles. (A) Representative epifluorescence images of 4T1 breast cancer cells incubated with FITC-labeled nanoparticles for defined time periods. The cells were counterstained with Lysotracker red dye. Merge images reveal colocalization after 6 hours persisting up to 24 hours. (B) Concentration efficacy graph showing effect of empty polymer, cisplatin nanoparticle and free cisplatin on 4T1 cell viability at 48 h. Data shown are mean SEM from n=3 independent experiments with triplicates in each experiment.

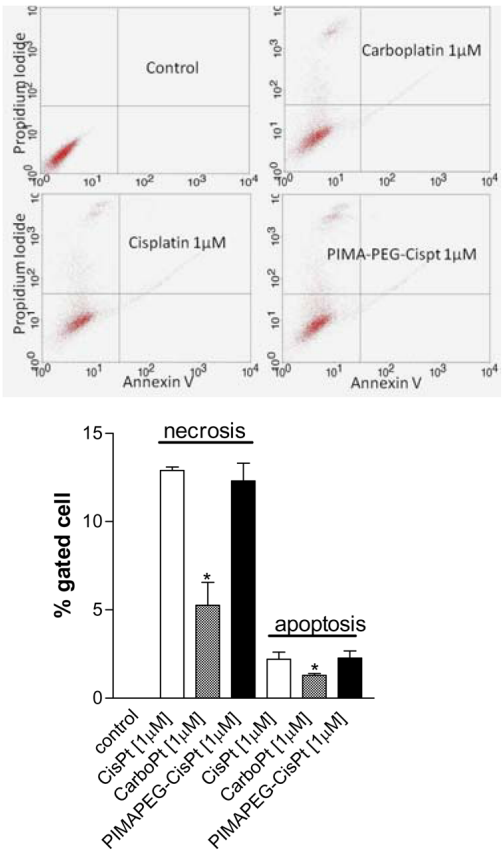

Figure 3.

Representative FACS scatter plots showing the mechanisms underlying cell death induced by free cisplatin, carboplatin or PIMA-PEG-Cisplatin nanoparticles. The cells were labeled with Annexin V-Alexa Fluor 488 and propidium iodide and then FAC-sorted. Graph shows the % of cells at each stage following different treatments. Data shown are mean ± SEM from n=3 (independent experiments).

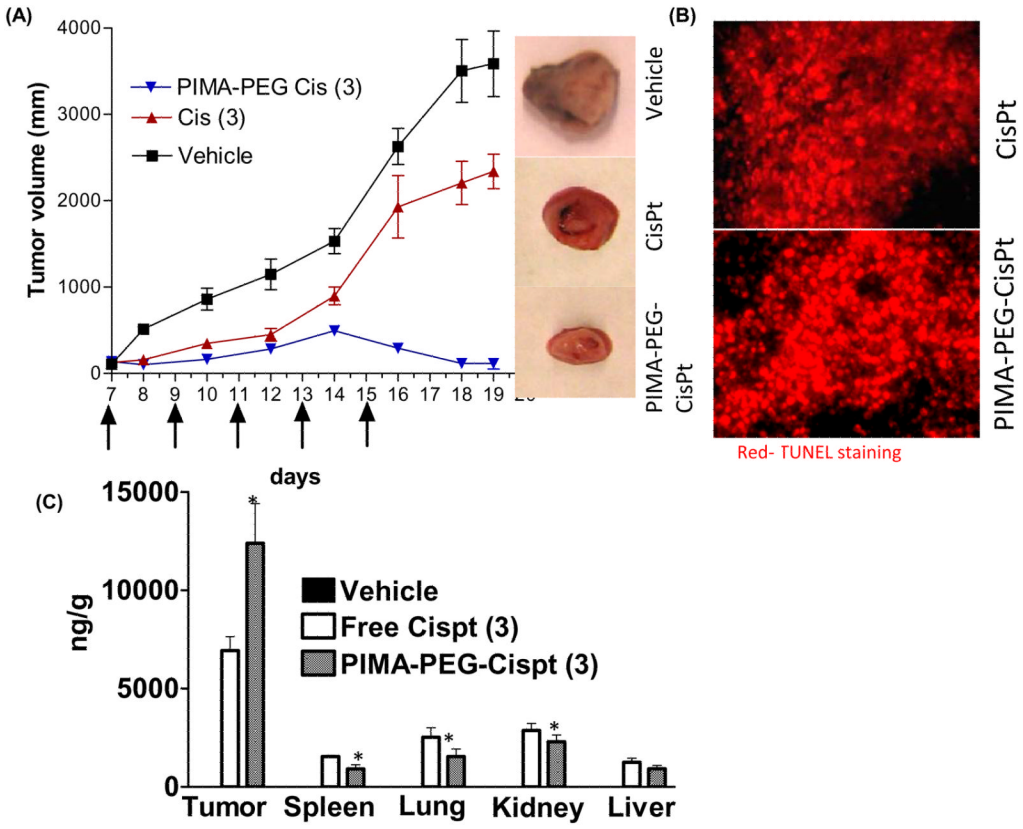

Figure 4.

In vivo efficacy of PEG-PIMA-Cisplatin nanoparticle in a syngeneic 4T1 murine breast tumor. (A) graph shows the tumor growth delay following treatment with free cisplatin (Cis) or cisplatin nanoparticle at 3mg/kg dose equivalent of cisplatin. The arrows depict the days on which the animals were injected with the drugs. (B) Cross-sections of tumors TUNEL-labeled for apoptosis. Low magnification (10×) images are shown to depict a large cross section. (C) Graph shows the biodistribution of platinum when administered as cisplatin or cisplatin nanoparticle. All data shown are mean ± SEM from n>4 per data point.

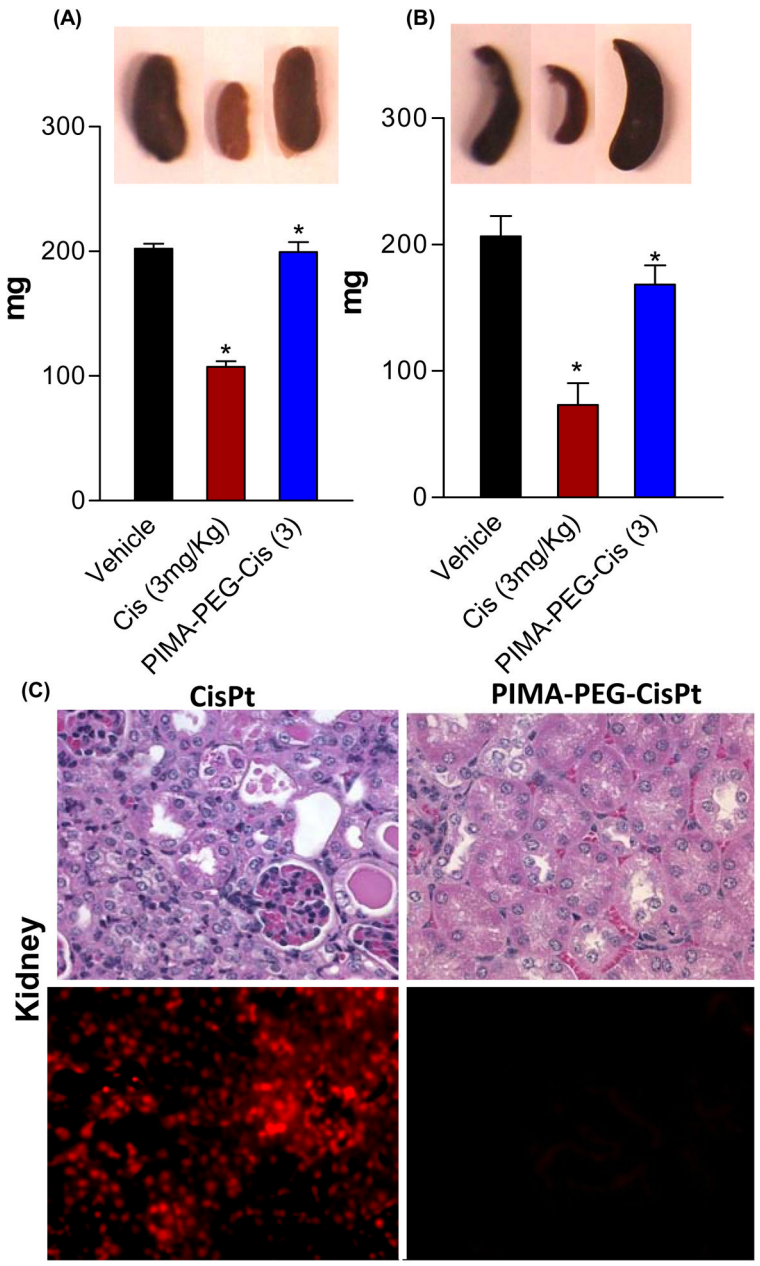

Figure 5.

(A-B) Graphs show effect of treatments on kidney and spleen weight respectively. (D) Representative images of kidney sections. Top panel is stained with H&E and bottom panel shows epifluorescence images of kidney sections stained for TUNEL. Data shown are mean ± SEM, with n>4 at each data point. *p<0.05 vs vehicle treated controls.